The Journal of the Astronautical Sciences (2024) 71:39
https://doi.org/10.1007/s40295-024-00457-4

ORIGINAL ARTICLE

Linear Polarization Signatures of Geosynchronous Satellites

Blake Eastman[1] · David Strong[2] · Francis Chun[1] · Daniel O'Keefe[1]

Accepted: 21 August 2024

Abstract
Space situational awareness (SSA) techniques must be developed to provide adequate understanding of the space environment. Optical techniques provide one mechanism to achieve this capability. Using a linear polarimeter mounted to a 16-inch telescope, the polarimetric signature of different satellites across different seasons was collected. These signatures reveal the degree of linear polarization (DOLP) and angle of linear polarization (AOLP) of the light reflected from observed satellites. Two features of geosynchronous satellite polarization signatures can be observed: a quadratic baseline originating from solar panels, and a polarization glint originating from the bus and payload. In demonstrating physical significance behind a satellite's polarization signature, these findings suggest satellite polarization may provide utility in identification and characterization of space objects.

Keywords Space situational awareness · Geosynchronous satellites · Polarization · Solar panels

1 Introduction

Space is becoming increasingly contested and congested as access becomes easier. Consequently, space situational awareness (SSA) techniques must be developed to provide adequate understanding of the space environment. The United States Air Force defines SSA as the "knowledge and characterization of space objects and the [operational environment] upon which space operations depend" [1]. As a result, the ability to identify and characterize satellites is fundamental to SSA. Optical measurements provide one mechanism to achieve this capability.

For small-aperture telescopes (1-m or less in diameter), resolved imaging of satellites is usually not viable [2]. As a result, efforts to optically characterize satellites

✉ Blake Eastman
blakeeastman1212@gmail.com

[1] Department of Physics and Meteorology, USAF Academy, CO 80840, USA

[2] Strong EO Imaging, Inc., Colorado Springs, CO 80908, USA

Published online: 18 September 2024

with small telescopes must rely on the satellite's unresolved optical signature. Much of the previous research involves photometry—the measurement of the brightness of the object as viewed through different colors filters [3–5], and slitless spectroscopy using transmission gratings to obtain the first order visual spectrum [6, 7]. Methods have demonstrated that optical signatures of satellites are consistent across nights and that the strong satellite glints originate from solar panels.

Photometry and spectroscopy provide information about a satellite's brightness over time (photometry) and wavelength profile (spectroscopy). A third measurement starting to gain traction for non-resolved satellite optical characterization is polarimetry. In simulations of satellite light signatures, incorporation of polarization into a bidirectional reflection distribution function has been shown to allow material property estimation [8]. By collecting the intensity of four different polarizations of light sequentially, but near-simultaneously, the degree and angle of linear polarization (AOLP) can be derived [9]. The polarization of reflected light provides additional insight into imaged objects, as it is a function of the index of refraction and the light's angle of incidence.

In this paper, we present the linear polarization signatures of several operational communication GEO satellites. We first describe the polarimeter and then present the features of a satellite's polarization signature, identifying whether its source is the solar panels or spacecraft bus itself.

2 The Polarimeter

To measure satellite polarization, an Andor Ulta U47 CCD camera is mounted to a 16-inch aperture f/8.2 Cassegrain telescope (USAFA-16). Between the camera and the telescope, a rotating filter wheel contains four linear polarization filters. These filters are oriented at either 0°, 45°, 90°, or 135° with respect to the focal plane of the camera. Only one filter is used at a time, and a collection of four images is used to generate one measurement of degree of linear polarization (DOLP) and AOLP. Figure 1 provides examples of images of GEO satellites taken through each of the four linear polarization filters. We note that the fourth stokes parameter, S_3, was not included in the research due to a limited number of slots available in the filter wheel.

The optical system alters the polarization of incident light before it is imaged. To correct for this, observations of light with known polarization were made. Using these observations, a calibration matrix was developed to convert the intensities of light at each orientation into the corresponding Stokes parameters of the source light [11]. Since the creation of the first calibration matrix, the polarimeter has been recalibrated at night, reducing the background in the process. The current calibration matrix for the USAFA-16 telescope is

$$W = \begin{pmatrix} 0.4885 & 0.4870 & 0.5105 & 0.5150 \\ 1.0363 & 0.0063 & -1.0495 & 0.0222 \\ 0.0635 & 1.0140 & 0.0367 & 1.0846 \end{pmatrix} \quad (1)$$

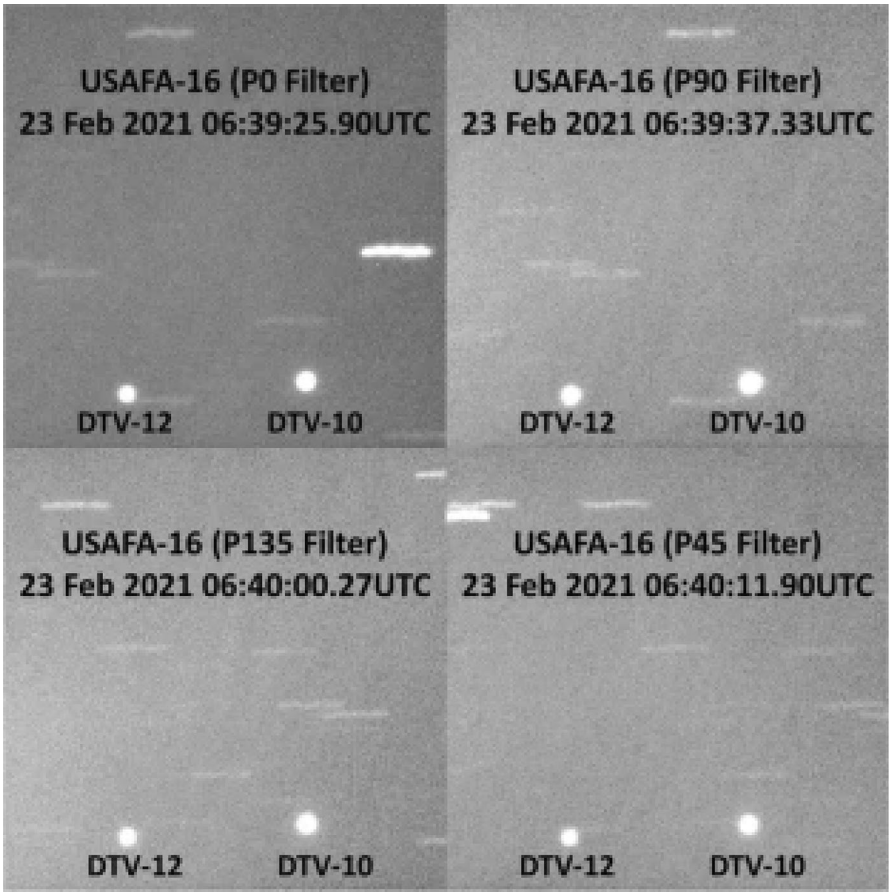

Fig. 1 GEO satellites imaged through the four different linear polarization filters using USAFA-16 [10]

where the rows indicate the stokes parameters (S_0, S_1, S_2), while the columns represent the four polarization angles (0°, 45°, 90°, 135°). The calibration matrix is then used to map the intensities of each of the four filters to the Stokes parameters, as shown in Eq. (2).

$$\begin{bmatrix} S_0 \\ S_1 \\ S_2 \end{bmatrix} = W \begin{bmatrix} I_0 \\ I_{45} \\ I_{90} \\ I_{135} \end{bmatrix} \tag{2}$$

Previous work showed that in images where there are multiple GEO satellites, each GEO should exhibit independent polarization signatures [12]. However, some nights, the GEOs in the same image show correlated polarization signatures (R^2 values of approximately 0.5 or greater). When this correlation occurs, we can conclude that the atmospheric conditions for that night's observations were less than ideal (i.e.

clouds were present), allowing us with the means to identify corrupted data and thus removing then from this study [12].

The Stokes parameters permit computation of two quantities: the DOLP and the angle of linear polarization (AOLP). The DOLP is defined as [13]

$$DOLP = \frac{\sqrt{S_1^2 + S_2^2}}{S_0} \tag{3}$$

and the AOLP is defined as

$$AOLP = \frac{1}{2}\tan^{-1}\left(\frac{S_2}{S_1}\right) \tag{4}$$

These two quantities are used to quantify and analyze the linear polarization signature of satellites.

3 Features of Satellite Polarization

3.1 Solar Panel Baseline

One feature present in the DOLP of satellite signals is a baseline curve that appears quadratic with respect to longitudinal phase angle (LPA). In order to quantify this baseline, a two-step process is used. First, any non-quadratic behavior at low phase angles is removed from the data by eliminating any data point between $-5°$ and $5°$ LPA, leaving only quadratic, non-glint data. Second, in order to remove microglints at high phase angles, any data that falls outside the 99% prediction interval of an initial fit is removed, and a second quadratic curve is fit to the remaining data. The purpose in removing outliers before finalizing the fit is to eliminate the effects of the glint or microglints on what is intended to be a characterization of the quadratic element of the polarization signature generated by the solar panels. Figure 2 provides a selection of polarization signatures observed from four different GEO satellites, as well as the quadratic behavior at higher phase angles.

This quadratic behavior in polarization aligns with expectations of solar panel polarization. Figure 3 provides polarization imaging of terrestrial solar panels, as well as an example of reflection coefficients of silica for two polarizations of light. In Fig. 3a, the DOLP of solar panels is lower when imaged at lower phase angles, aligning with the behavior of the quadratic fit. Furthermore, as shown in Fig. 3b, the reflection coefficients demonstrate that, at phase angles lower than the Brewster's angle, the amount of reflection between two different polarizations begins to separate as phase angle increases. This separation indicates an increasing polarization of reflected light. This behavior is consistent with the observed quadratic in satellite polarization curves.

Another feature of the solar panel polarization in Fig. 3a is a shift in AOLP observed across zero phase angle. As further confirmation that the origin of the observed quadratic is satellite solar panels, Fig. 4 provides both DOLP and AOLP

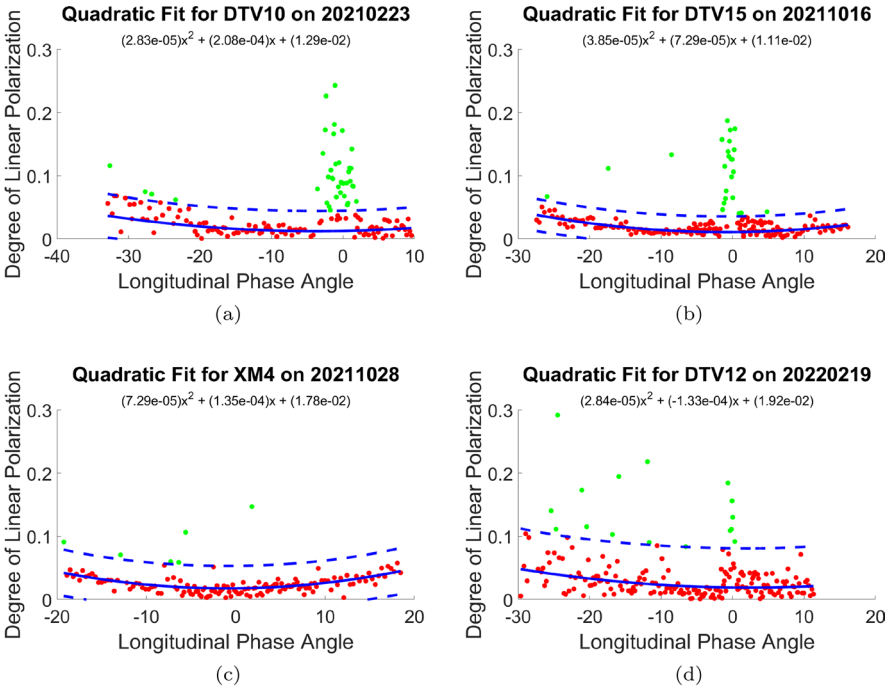

Fig. 2 Polarization of **a** DirecTV 10 on 23 February 2021, **b** DirecTV 15 on 16 October 2021, **c** XM4 on 28 October 2021 and **d** DirecTV 12 on 19 February 2022. The solid blue line shows the quadratic fit, while the dashed lines cover the prediction interval. Red data fall within the predicted quadratic polarization, while green data do not

for DTV15 and MEXSAT3 during the fall 2021 glint season. Correspondingly, the DOLP quadratic is still observable, while the AOLP has a distinct shift as the satellite crosses zero phase angle. The correspondence between the quadratic behavior of satellite polarization signatures and the polarization signatures of solar panels, indicates that the second order baseline of satellite polarization emerges from satellite solar panels.

The predictability of solar panel polarization may allow identification of signals that do not correspond to a satellite's solar panels. Analysis of signals that fall outside the prediction interval of the quadratic curve may provide insight into other sources of polarization signal on the satellite, offering a potential method to identify components of the payload or bus. Furthermore, differences in non-quadratic signals between nights of observation may indicate changes to the satellite's geometry. Ultimately, however, these results demonstrate that there is physical significance behind the shape of a satellite's polarization signature. Table 1 provides the fit parameters for various satellites' quadratic behavior.

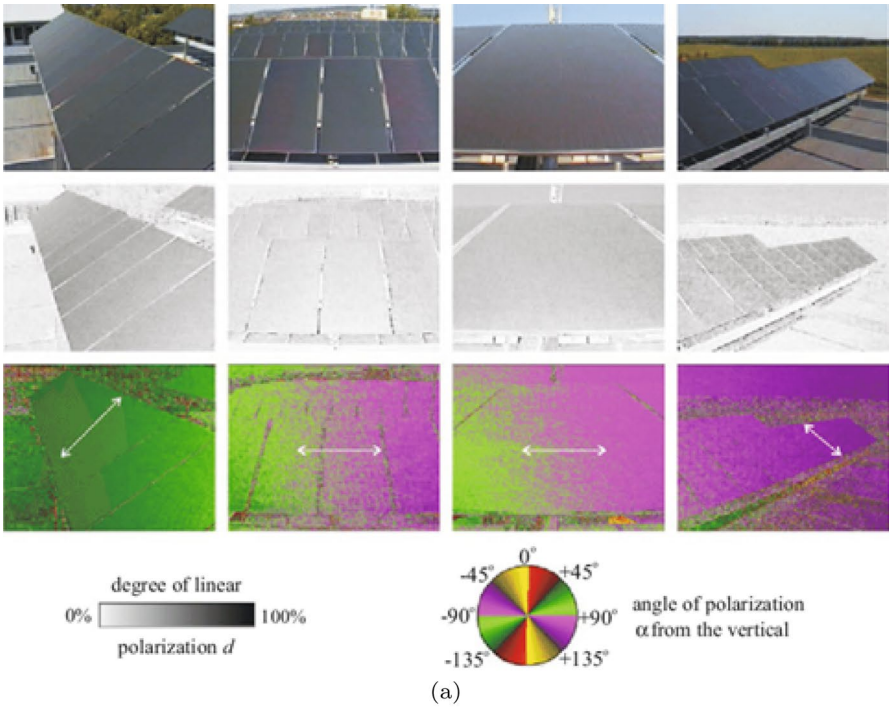

(a)

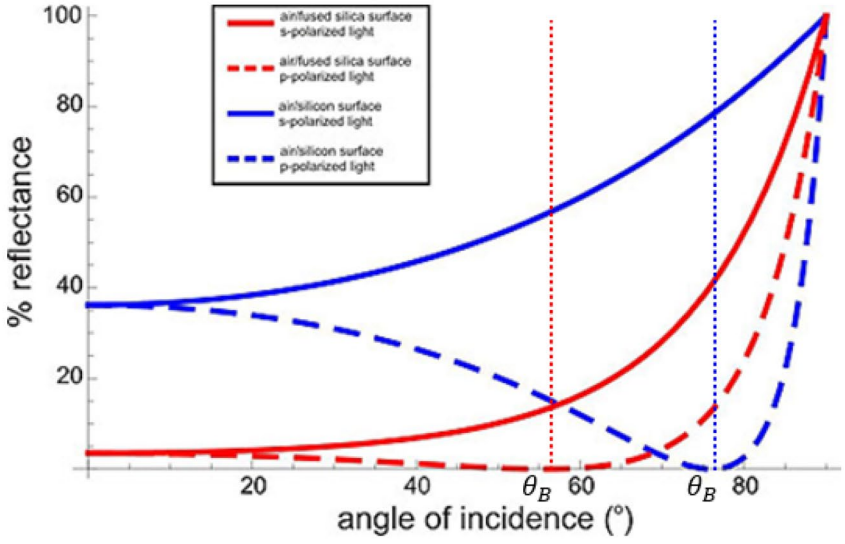

(b)

Fig. 3 **a** Polarization signature of terrestrial solar panels at different phase angles. The top row presents the true color image, the middle row presents DOLP, and the bottom row presents AOLP. [14]. **b** Percent of light reflected from silica by phase angle (angle of incidence) [15]. The Brewster's angle for each material is labeled as θ_B

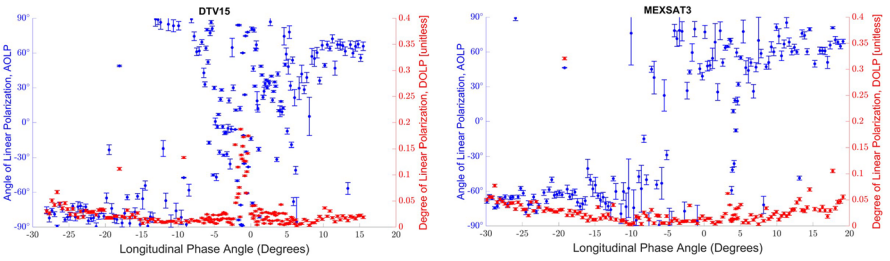

Fig. 4 Angle and DOLP for **a** DirecTV 15 on 16 October 2021 and **b** Mexsat 3. DOLP is provided in red, while AOLP is provided in blue

Table 1 Quadratic fit parameters for each satellite

Name	Date	Quadratic	Linear	Constant
DirecTV 10	23 February 2021	2.8350e−05	2.0820e−04	1.2878e−02
DirecTV 10	16 October 2021	4.0581e−05	1.0594e−04	1.2618e−02
DirecTV 10	19 February 2022	6.5400e−05	5.1746e−04	1.6115e−02
DirecTV 12	23 February 2021	4.4340e−05	4.5513e−04	1.6876e−02
DirecTV 12	16 October 2021	4.8410e−05	3.0991e−04	1.4171e−02
DirecTV 12	19 February 2022	2.8440e−05	− 1.3282e−04	1.9183e−02
DirecTV 15	16 October 2021	3.8500e−05	7.2850e−05	1.1147e−02
DirecTV 15	28 October 2021	7.2910e−05	1.3492e−04	1.7787e−02
DirecTV 15	19 February 2022	4.6280e−05	2.5987e−04	1.5035e−02
MEXSAT 3	29 October 2021	4.6990e−05	3.2318e−04	1.3679e−02

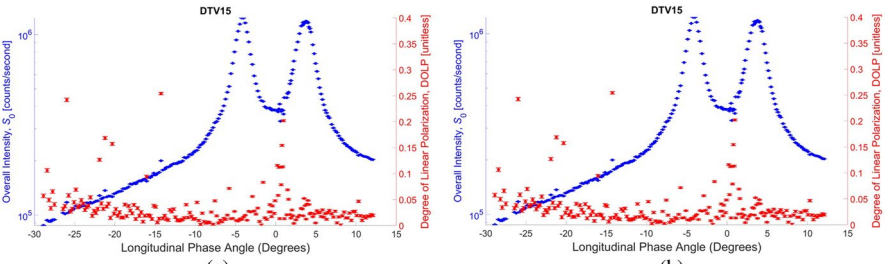

Fig. 5 Intensity and polarization of light for DirecTV 15 on **a** 20 February 2022 and **b** 16 October 2021. Intensity of light is in blue, while DOLP is in red

3.2 Spacecraft Bus Polarization

Apparent in some polarization signatures is a distinct increase in DOLP as a satellite passes through minimum phase angle. This polarization glint is not attributable to satellite solar panels, as it occurs when the polarization signal from solar panels should be at its minimum. Furthermore, in some observations (provided

in Fig. 5), the phase angles of the polarization glint is separated from the phase angle of maximum intensity, suggesting that the increase in polarization does not originate from the solar panels, but rather from the satellite bus or payloads.

To characterize the polarization glint, a normal distribution is fitted to the data after subtracting the quadratic baseline. The signal provided by a polarization glint is not necessarily normally distributed, so the fit is intended to serve as a quantification of polarization glint width and height, rather than as a prediction of measurements during the glint. Application of this technique to DirecTV 10 and DirecTV 12 is shown in Fig. 6. Despite these satellites being similar, their polarization glints show different characteristics. The maximum polarization of both satellite's glints is the same, but the duration of the glints differ. The equivalence of maximum polarization conforms with the material similarities between the

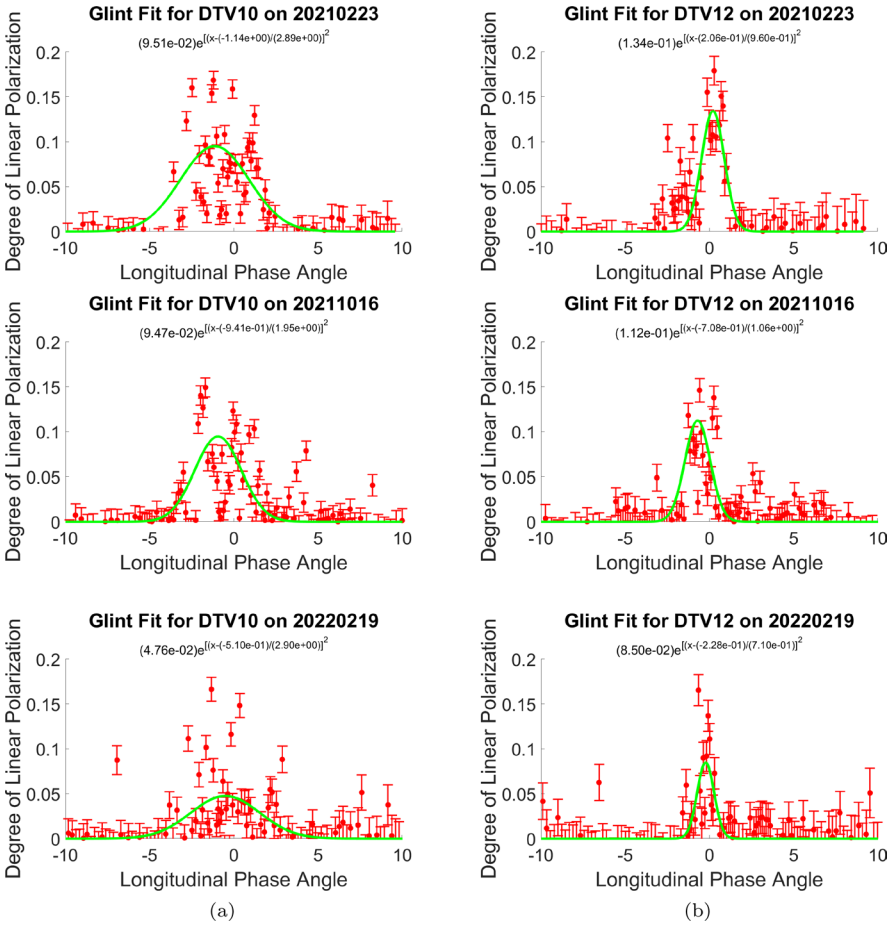

Fig. 6 **a** Three nights of polarization signatures for DirecTV 10. **b** The same three nights of polarization signatures for DirecTV 12. In each figure, the quadratic baseline is removed from the DOLP, and the Gaussian characterization is plotted

satellites; the polarization signature is generated from the same materials in both cases. However, the differences between the width of the polarization glints of these two satellites suggest that the polarization glint also depends on the angles formed between the sun, satellite surfaces and appendages, and observation site.

In Fig. 6, the polarization glint width appears consistent for the same satellite across different nights and seasons of observation. Because the compared satellites are identical in construction, yet present different glint structures, the consistency across nights is suggestive of a geometric origin to this consistency. Specifically, these communication satellites have likely not reoriented any payload or bus surfaces, so they appear consistent in their polarization signature. The physical interpretation of the polarization signatures measured offers a means to use polarization to detect changes in a satellite's configuration. Accordingly, measurement of satellite polarization glints offers potential utility in SSA. Table 2 provides the fit parameters for several satellites' glints.

4 Conclusion

Despite only being able to observe the unresolved signature of operational GEO satellites (Fig. 1), the linear polarization signature of those satellites contains two distinct features: a quadratic baseline as well as a polarization glint. The quadratic baseline enables discrimination between polarization signals originating from the solar panel and other sources. The polarization glint originates from the satellite bus or payload, and its height and width differ according to both satellite bus/payload material and geometry. These findings represent the first known experimental demonstration that satellite features can be distinguished in a polarization signature.

When a component of the signature behaves non-quadratically, the component most likely corresponds to signals from a source other than the satellite solar panels. Comparison between non-quadratic components of the satellite's polarization signature across nights of observation offers a tool to detect changes in the satellite.

Table 2 Polarization glint characteristics for various satellites

Satellite	Date	Maximum DOLP	Peak angle	Width
DirecTV 10	23 February 2021	0.0951	− 1.1385	2.8873
DirecTV 10	16 October 2021	0.0946	− 0.9417	1.9517
DirecTV 10	19 February 2022	0.0475	− 0.5111	2.9019
DirecTV 12	23 February 2021	0.1343	0.2059	0.9593
DirecTV 12	16 October 2021	0.1123	− 0.7105	1.0613
DirecTV 12	19 February 2022	0.0850	− 0.2280	0.7099
DirecTV 15	16 October 2021	0.1246	− 0.3447	1.0583
DirecTV 15	19 February 2022	0.0943	0.7499	0.7270
XM4	28 October 2021	3.1797	0.1340	0.0066
MEXSAT 3	29 October 2021	− 0.0103	1.5942	0.5909

If a satellite is no longer reflecting light in the same way as it had in the past, it has changed in some way. Future work continues in exploring ways to extract specific, useful information about changes to a satellite from observed changes in its signature.

Furthermore, better utilization of polarization measurement may be possible by combining polarization and hyperspectral measurement. By collecting both color and polarization information simultaneously, it may be possible to isolate the polarization signal of various different reflecting surfaces, by considering the polarization of specific wavelengths of light. For instance, the polarization of blue reflected wavelengths is likely dominated by the solar panels. A new 1-meter telescope at the United States Air Force Academy was recently installed, featuring two filter wheels. Additionally, the Falcon Telescope Network is being upgraded to also include dual filter wheels. Future work on satellite polarimetry will explore the combination of a polarimeter and a diffraction grating to explore the possibility of making material characterizations of satellites.

Primarily, the findings presented here provide an experimental demonstration that the polarization signature of a satellite contains features which can be identified with different parts of the satellite. Additionally, other work has shown that material properties of a satellite can be estimated using multiple-model adaptive estimation on a polarized bidirectional reflection distribution function [8]. The combination of these lines of evidence suggest that a viable method for satellite characterization and change detection in SSA can be developed through observation of satellite polarization signatures.

Acknowledgements We want to acknowledge the support of the Air Force Office of Scientific Research.

Data availability The data is not available.

Declarations

Conflict of interest The authors have no financial interests or potential conflict of interest to disclose.

References

1. Scott, K.: Joint publication 3-14: Space operations. US Chairman of the Joint Chiefs of Staff Technology Report 10 (2018)
2. Fulcoly, D.O., Kalamaroff, K.I., Chun, F.K.: Determining basic satellite shape from photometric light curves. J. Spacecr. Rocket. **49**(1), 76–82 (2012)
3. Payne, T.E., Gregory, S.A., Houtkooper, N.M., Burdullis, T.W.: Classification of geosynchronous satellites using photometric techniques. In: Proceedings of the 2002 AMOS Technical Conference, pp. 353–362. Maui Economic Development Board, Inc. Kihei, Maui (2002)
4. Payne, T., Gregory, S., Luu, K.: SSA analysis of geos photometric signature classifications and solar panel offsets. In: The Advanced Maui Optical and Space Surveillance Technologies Conference, p. 73 (2006)
5. Vrba, F.J., DiVittorio, M.E., Hindsley, R.B., Schmitt, H.R., Armstrong, J.T., Shankland, P.D., Hutter, D.J., Benson, J.A.: A survey of geosynchronous satellite glints. Technical report, Naval Observatory, Flagstaff (2009)

6. Schildknecht, T., Vannanti, A., Krag, H., Erd, C.: Reflectance spectra of space debris in GEO. In: Advanced Maui Optical and Space Surveillance Technologies Conference, p. 24 (2009)
7. Dunsmore, A.N., Key, J.A., Tucker, R.M., Weld, E.M., Chun, F.K., Tippets, R.D.: Spectral measurements of geosynchronous satellites during glint season. J. Spacecr. Rocket. **54**(2), 349–355 (2017)
8. Dianetti, A.D., Crassidis, J.L.: Resident space object characterization using polarized light curves. J. Guid. Control. Dyn. **46**(2), 246–263 (2023)
9. Zimmerman, L., Chun, S., Pirozzoli, M., Plummer, M., Chun, F., Strong, D.: Near-simultaneous polarization and spectral optical measurements of geosynchronous satellites. In: The 2020 AMOS Technical Conference Proceedings, The Maui Economic Development Board, Inc., Kihei, Maui (2020)
10. Albrecht, E.M., Jensen, A.M., Jensen, E.G., Wilson, K.A., Plummer, M.K., Key, J.A., O'Keefe, D.S., Chun, F.K., Strong, D.M., Schuetz-Christy, C.P.: Near-simultaneous observations of a geosynchronous satellite using two telescopes and multiple optical filters. J. Astronaut. Sci. **69**(1), 120–138 (2022)
11. Pirozzoli, M.F., Zimmerman, L.A., Korta, M., Scheppe, A.D., Jensen, A.M., Strong, D.M., Plummer, M.K., O'Keefe, D.S., Chun, F.K.: Calibration, sensitivity analysis, and demonstration of a basic polarimeter for artificial satellite observations. Adv. Space Res. **69**(1), 581–591 (2022)
12. Jensen, A.M., Plummer, M.K., O'Keefe, D.S., Chun, F.K., Strong, D.M.: Observations of satellites using near-simultaneous polarization measurements. In: The Advanced Maui Optical and Space Surveillance Technologies Conference (2021)
13. Born, M., Wolf, E.: Principles of Optics. Cambridge University Press, Cambridge (2019)
14. Horváth, G., Kriska, G., Robertson, B.: Anthropogenic polarization and polarized light pollution inducing polarized ecological traps. In: Polarized Light and Polarization Vision in Animal Sciences, pp. 443–517. Springer, Berlin (2014)
15. Fink, M.C.: The polarization of light by Reflection (2008). https://www.photonics.com/Articles/The_Polarization_of_Light_by_Reflection/a35808